Journal of Inorganic and Organometallic Polymers and Materials (2019) 29:1503–1513
https://doi.org/10.1007/s10904-019-01114-2

Poly (ε-caprolactone) Microsphere Decorated with Nano-ZnO Based Phytoformulation: A Promising Antimicrobial Agent

S. Snigdha[1] · M. Rahul[2] · Nandakumar Kalarikkal[1,3] · Sabu Thomas[1,4] · E. K. Radhakrishnan[2]

Received: 8 January 2019 / Accepted: 21 February 2019 / Published online: 9 March 2019

Abstract
In this study, an ethnonanocomposite was produced by using *Curcuma zedoaria* and ZnO nanoparticles. This was immobilised on poly (ε-caprolactone) (PCL) microspheres for effective delivery. The presence of curcuminoids in *C. zedoaria* extract was confirmed by GC–MS and LC–MS analyses. The ZnO/*C. zedoaria*. nanocomposite synthesised in this study was subjected to X-ray diffraction and field emission scanning electron microscopy, which revealed the crystalline nature of formed nanocomposite. The nanocomposite was then immobilised on PCL microspheres by emulsion solvent evaporation. Further, XRD and FE-SEM confirmed the presence of nanocomposites and the spherical nature of the polymeric microspheres with diameter ranging from 4 to 36 µm. The antimicrobial activity analysis revealed the remarkable effectiveness of the nanocomposite loaded microspheres. The ethnonanocomposite loaded PCL microspheres generated in the study can thus be an effective antimicrobial agent with diverse biomedical applications.

Keywords *Curcuma zedoaria* · Nano-phyto formulation · Antimicrobial · Polymer microsphere · PCL microsphere · Ethnic-nanomedicine

1 Introduction

The quest for antimicrobial agents has been going on for centuries and hence nanotechnological exploration of ethnomedicine offers great promise. *Curcuma zedoaria* has been well documented in ethnic pharmacotherapy [1]. It has been known for its antibacterial as well as fungicidal properties. Moreover, it has shown pronounced analgesic, anti-oxidant, anti-tumor, and anti-clastogenic properties [2]. The dark orange colored rhizhome contains several active ingredients that are highly sought out among traditional medicine practitioners [3]. With the alarming increase in antibiotic resistance among pathogens, an emerging interest to explore the efficiency of age-old herbal remedies through nanotechnological methods has evolved [4, 5]. Such combinatorial therapeutics are likely to possess multi-targeting capabilities against pathogenic microbes and could hold great potential in managing drug resistant pathogens.

Metal nanoparticles have been established as effective antimicrobial agents [6–10]. In this study, ZnO NPs with well known antimicrobial and anti-inflammatory properties were selected to develop nanoparticle-based phytomedicine [11, 12]. ZnO NPs have proved to be highly efficient in conjugation with materials of plant origin [13–15]. The ZnO NPs have superior effect to eradicate microbes at significantly low concentration. By using a carrier to house ZnO NPs, a small amount of material can be effectively delivered to the target site [16, 17]. PCL has proved its versatility in biomedical applications over the past few decades [18–20]. PCL has been used to immobilise nanoparticles, bioactive agents, enzymes as well as live cells [21, 22]. It has also been engineered into various morphologies according to the need for delivery of the therapeutic materials. For this, PCL has been converted into electrospun mats, cast into thin films, freeze dried into monoliths, 3D printed, and emulsified into nano/microparticles [23–25]. Biocompatible

✉ E. K. Radhakrishnan
radhakrishnanek@gmail.com; radhakrishnanek@mgu.ac.in

1 International and Inter University Centre for Nanoscience and Nanotechnology, Mahatma Gandhi University, Kottayam 686 560, India

2 School of Biosciences, Mahatma Gandhi University, Kottayam 686 560, India

3 School of Pure and Applied Physics, Mahatma Gandhi University, Kottayam 686 560, India

4 School of Chemical Sciences, Mahatma Gandhi University, Kottayam 686 560, India

polymeric nanoparticles have been extensively prepared and applied for various biomedical purposes [26–29].

The current study reports the preparation of a novel phytoformulation with microbicidal properties using *C. zedoaria*, complexed with ZnO nanoparticles. The phytoformulation was further loaded onto polymer microspheres for effective delivery of the antimicrobial composite. The biocompatibility, biodegradability and stability of PCL along with the unique features of the phytonanoformulation make the study significantly important.

2 Materials and Methods

2.1 Preparation of Crude Extract

Fresh *C. zedoaria* rhizomes were acquired from Indian Institute of Spices Research, Kozhikode, Kerala, India. The collected rhizomes were cleaned, steamed for 7 min and sliced into small pieces before drying in a hot air oven at 50 °C for 6 h. The dried material was collected and ground into fine powder using a high-speed blender. The dry, ground rhizome was used for further study [3].

2.2 Preparation of Sample

The finely powdered rhizome sample (0.3 g) was extracted using 30 mL of methanol in a probe sonicator at 35 kHz for 60 min at room temperature. The solution was filtered using a 0.22 µm syringe filter and the residue was treated with 20 mL methanol and mixed well. This was filtered using Whatman filter paper no: 1, and finally filtered using 0.22 µm syringe filter [30].

2.3 Development of Nanoparticle Based Conjugate of *C. zedoaria* Extract

2.3.1 Selection of Nanoparticles

ZnO NPs were purchased from Sigma Aldrich, India. The ZnO nanoparticles specifications were as follows: TEM particle size: < 100, average particle size: < 40 nm. ZnO was selected due to its excellent antimicrobial activity in association with phytochemicals.

2.3.2 Preparation of Nanoparticle Samples

ZnO nanoparticles in water was prepared at a concentration of 1 mg/mL. *C. zedoaria* extract (1 mL) was mixed with the nanoparticle solution at 1:1 ratio and sonicated for 4 h at 35 kHz for 60 min at room temperature to produce the nanoconjugate. The mixture was then filtered using a Whatman filter paper no: 1 and stored at 4 °C.

2.4 Preparation of PCL Microspheres Loaded with ZnO/*C. zedoaria nanocomposite*

The PCL microspheres loaded with ZnO/*C. zedoaria* nanocomposite was prepared using W/O/W emulsion solvent evaporation technique (Fig. 1). Polycaprolactone (PCL) (MW ~ 80,000) was purchased from Sigma Aldrich, St. Luis, USA. Dichloromethane (DCM) (purity ~ 99.5%) was purchased from Himedia, India. Polyvinyl Alcohol (PVA) (MW ~ 92,500) was purchased from Himedia, India. 1% solution of PVA in water was prepared and stored until further use. The PCL beads (100 mg) were dissolved in 10 mL of DCM. To the polymer solution, 3 mL of aqueous medium containing ZnO-*C. zedoaria* was added and

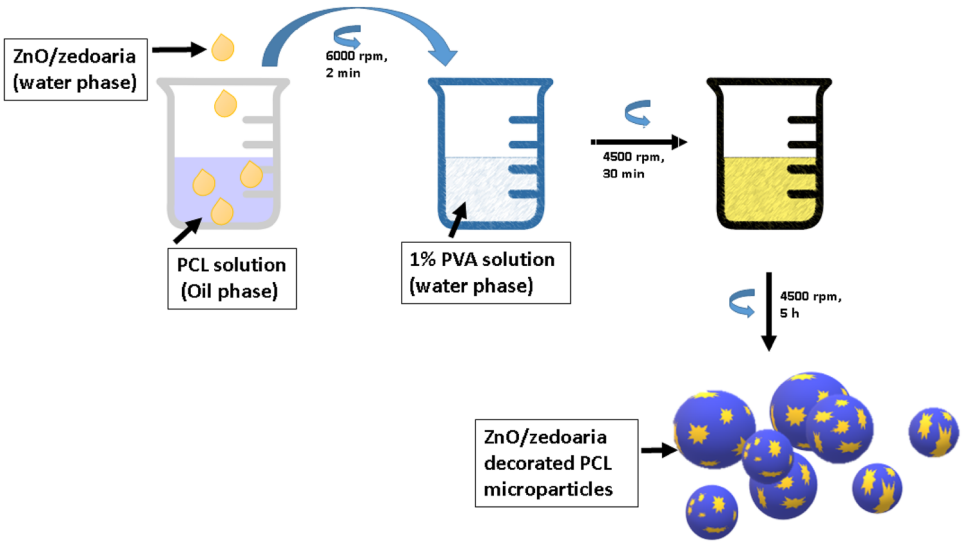

Fig. 1 Schematic representation of the PCL microsphere preparation using the W/O/W emulsion solvent evaporation technique

stirred vigorously at 6000 rpm for 2 min. This emulsion was then introduced into 30 mL of aqueous phase containing PVA (1%), and stirred at 4500 rpm for 150 min at 30 °C. The solution was further stirred for 5 h at 30 °C in order to evaporate the residual DCM. Complete evaporation of the organic solvent resulted in polymer hardening and eventual entrapment of the phytoformulation on the polymer [31]. The procedure for preparation of PCL microspheres has been schematically presented in Fig. 1.

3 Characterization Techniques

3.1 Metabolite Analysis of the Crude Extract

3.1.1 Gas Chromatography Mass Spectrometry (GC–MS)

GC–MS was carried out to analyse and identify the active ingredients in the prepared extract. GC–MS analysis was carried out using Shimadzu GC–MS System model number QP 2010S. The filtered and diluted rhizome extract (1 µL) was injected into the GC system provided with 30 m × 250 µm × 0.25 µm Rxi-5Sil MS column. Helium was used as the carrier gas with a column flow rate of 1.00 mL/min. The GC oven was held at 80 °C and then ramped from 80 to 260 °C at 5 °C/min. The chromatogram and mass spectra were recorded and analysed [32].

3.1.2 Liquid Chromatography Mass Spectrometry (LC–MS)

Filtered extract was also used for metabolite analysis by liquid chromatography–mass spectrometry using Acquity H Class (Waters, Milford, MA, USA) ultra performance liquid chromatography with BEH C18 column (50 mm × 2.1 mm × 1.7 µm) and a Xevo G2 (Waters) mass spectrometer. A mixture of methanol and water was used as mobile phase and was delivered at a flow rate of 0.3 mL/min for a scan time of 9 min. The source temperature and desolution temperature were 135 and 350 °C respectively. The capillary voltage of 3 kV was used [32].

3.2 UV–Vis Spectroscopy

For the characterization of prepared ZnO-zedoaria conjugate, UV–Vis absorbance spectrum analysis was conducted using a Shimadzu UV 2600 142 spectrophotometer in the range 200–700 nm at a resolution of 1 nm [33].

3.3 X-ray Diffraction (XRD)

XRD measurements for all the samples were carried out in Bruker D8 Advance X-Ray Diffractometer with nickel-filtered CuKα radiation operating at 45 kV and 44 Ma, with minimum step size 2θ: 0.001° and ω: 0.001°; divergence and receiving Slit Size of 0.4354 and 0.3000 mm respectively. All data were collected in the 2θ range of 2°–40° with a scanning rate of 5°/min. XRD was carried out on purified and dried samples [33].

3.4 Field Emission-Scanning Electron Microscopy

The surface morphology of the prepared nanocomposite was investigated with the help of FE-SEM. The purified nanocomposite was air dried and sputter coated with gold.

The morphology of the prepared polymer microspheres was investigated with the help of FE-SEM. The purified microspheres were air dried and sputter coated with gold. The gold coated samples were imaged using Carl Zeiss SIGMA FE-SEM at an accelerating voltage of 3 kV.

3.5 Antimicrobial Properties

The prepared nanocomposite formulation was assayed for antibacterial activity against *S. aureus*. For this, the test organism was inoculated into 10 mL of nutrient broth and was incubated overnight at 37 °C. For the antimicrobial activity analysis, Mullen Hinton (MH) agar plates were used. The test organism was swabbed onto the surface of the MH agar plates. To the individual wells made on the agar, 60 µL each of methanol (control), nanoparticle, plant extract, and nanoformulation were introduced.

The antimicrobial activity of the prepared polymer microspheres was analysed against *S. aureus* as explained earlier. Two wells were punched on the agar, one each for neat and ZnO/*C. zedoaria* nanocomposite loaded PCL microspheres respectively. The test organism was then swabbed uniformly on the surface of agar plate. To each well, 60 µL of the respective microspheres were introduced. This study was performed in triplicate. All the plates were incubated at 37 °C [34].

4 Results and Discussion

Phytoformulations have increasing demand due to their low toxicity and easy availability. At the same time, nanostructured materials have been highly desirable for microbicidal applications due to their ability to penetrate into cells with ease. Therefore, a combination of an ethnopharmacological material and a metal oxide NP for antimicrobial applications can be considered highly potent due to their multi-targeted activity.

4.1 Metabolite Analysis of the Crude Extract of *C. zedoaria*

The *C. zedoaria* crude extract was subjected to metabolite profiling by GC–MS and LC–MS, in order to confirm the active ingredients in the extract.

4.1.1 Gas Chromatography Mass Spectrometry (GC–MS)

GC–MS analysis detected the presence of α-curcumene, β-curcumene, and δ-cuparenol as the major compounds from the extract of the *C. zedoaria* (Fig. 2; Table 1) [35]. These three compounds are well known for their anti-inflammatory and antimicrobial properties [36].

4.1.2 Liquid Chromatography Mass Spectrometry (LC–MS)

The LC–MS analysis of crude extract indicated the presence of various compounds (Fig. 3a). Thus elution peak of *C. zedoaria* extract at 6.31 min, upon ionisation and mass spectrometry revealed the presence of curcuminoid derivatives (Fig. 3a, b). The deprotonated ions $[M–H]^-$ of particular interest in this study were found to have m/z values of 367, 337 and 307 (Fig. 3b). These indicated the presence of curcuminoids in the extract. Further these were subjected to MS/MS analysis which showed these molecular ions to have daughter ions with m/z values of 217, 173, 149 for 367 (Fig. 3c), 217 and 173 for 337 (Fig. 3d), and 182 & 148 for 307 (Fig. 3e) respectively. The molecular ion with m/z value 367 indicated the presence of curcumin, 337 that of demethoxy curcumin and 307 of bisdemethoxycurcumin. Thus the presence of the curcuminoids could be confirmed in the extract as major metabolites by GC–MS and LC–MS [37–39]. These curcuminoids have already been demonstrated for their antimicrobial activity [40]. The presence of these diverse metabolites could be predominantly responsible for the antimicrobial properties exhibited by the *C. zedoaria* extract.

4.2 Characterization of Nanoconjugate

4.2.1 X-ray Diffraction (XRD)

The reflections for ZnO NPs can be observed at 2θ = 31.6°, 34.2°, 36.1°, 47.4°, 56.5°, 62.7°, 66.3°, 67.8°, and 68.9°. These represent hexagonal wurtzite phase of ZnO with lattice constants $a = b = 0.324$ nm and $c = 0.521$ nm (JPCDS number: 36-1451). The high intensity reflections between 30° and 40° are indicative of highly crystalline regions in the nanoparticles. The XRD diffraction patterns exhibited by extract of *C. zedoaria* showed the presence of reflections at 2θ = 14.5°, 17.2°, 21.17°, 23.47° and 25.5°. The presence of sharp reflections between 10° and 30°, could refer to the presence of crystallite structures in the extract. The nanocomposite ZnO/*C. zedoaria* XRD profile showed the reflections of both ZnO nanoparticles and *C. zedoaria* as well (Fig. 4) [13, 34]. The reflections of *C. zedoaria* can be observed from 2θ = 10° to 2θ = 30° and the major reflections of ZnO can also be observed in the ZnO/*C. zedoaria* XRD profile. The presence of highly crystalline ZnO nanoparticles was confirmed by XRD. The XRD profile of *C. zedoaria* extract revealed reflections comparable to those of curcumin. As the presence of curcuminoids in *C. zedoaria* extract was previously confirmed by GC–MS and LC–MS analyses, the XRD results can be concluded as indicative of presence of curcuminoids [41].

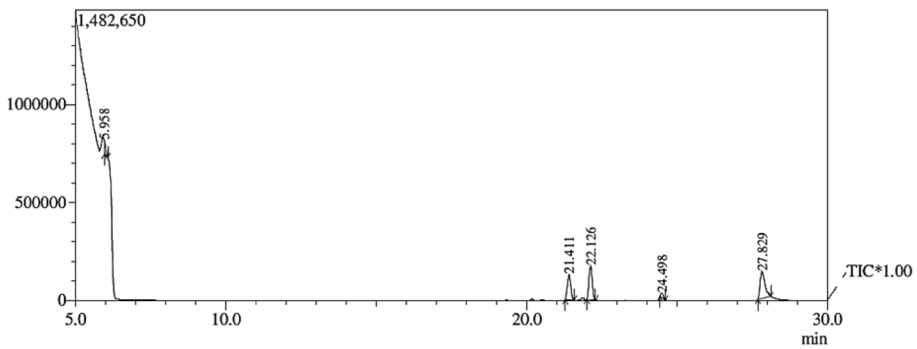

Fig. 2 GC–MS analysis of *C. zedoaria* extract

Table 1 Compounds of interest identified through the GC–MS analysis

Peak	R time	Area	Area %	Height	Height %	Name	Base m/z
2	21.411	978,049	5.43	130,195	11.2	α-Curcumene	119.15
3	22.126	1,288,522	7.16	174,634	15.05	β-Curcumene	119.15
5	27.829	1,506,412	8.37	140,676	12.12	Delta-cuparenol	136.15

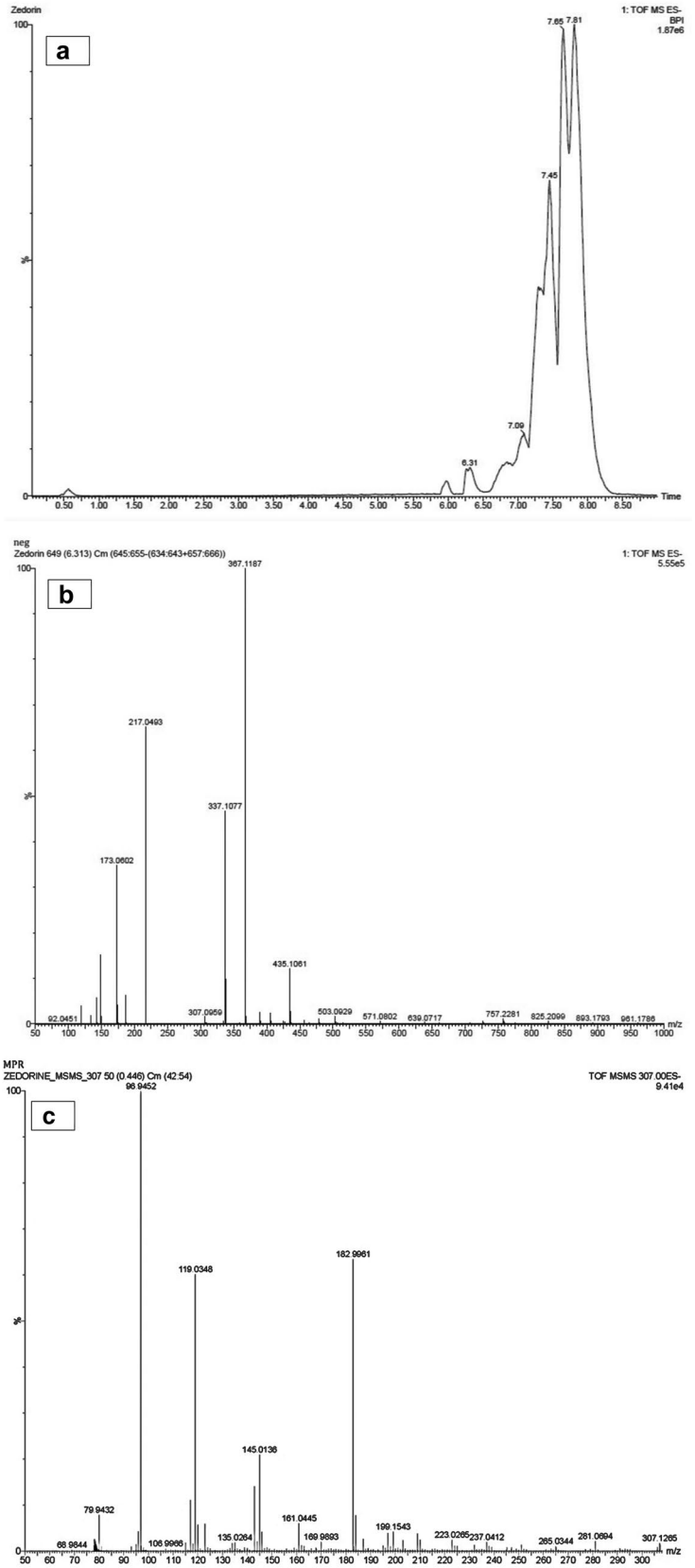

Fig. 3 Total ion chromatogram (TIC) of *C. zedoaria* extract (**a**), full scan spectra of the elution peak at 6.31 min, showing the curcuminoids (**b**) mass spectra of deprotonated ions of bis-demethoxycurcumin (307) (**c**), demethoxycurcumin (337) (**d**), and curcumin (367) (**e**)

Fig. 3 (continued)

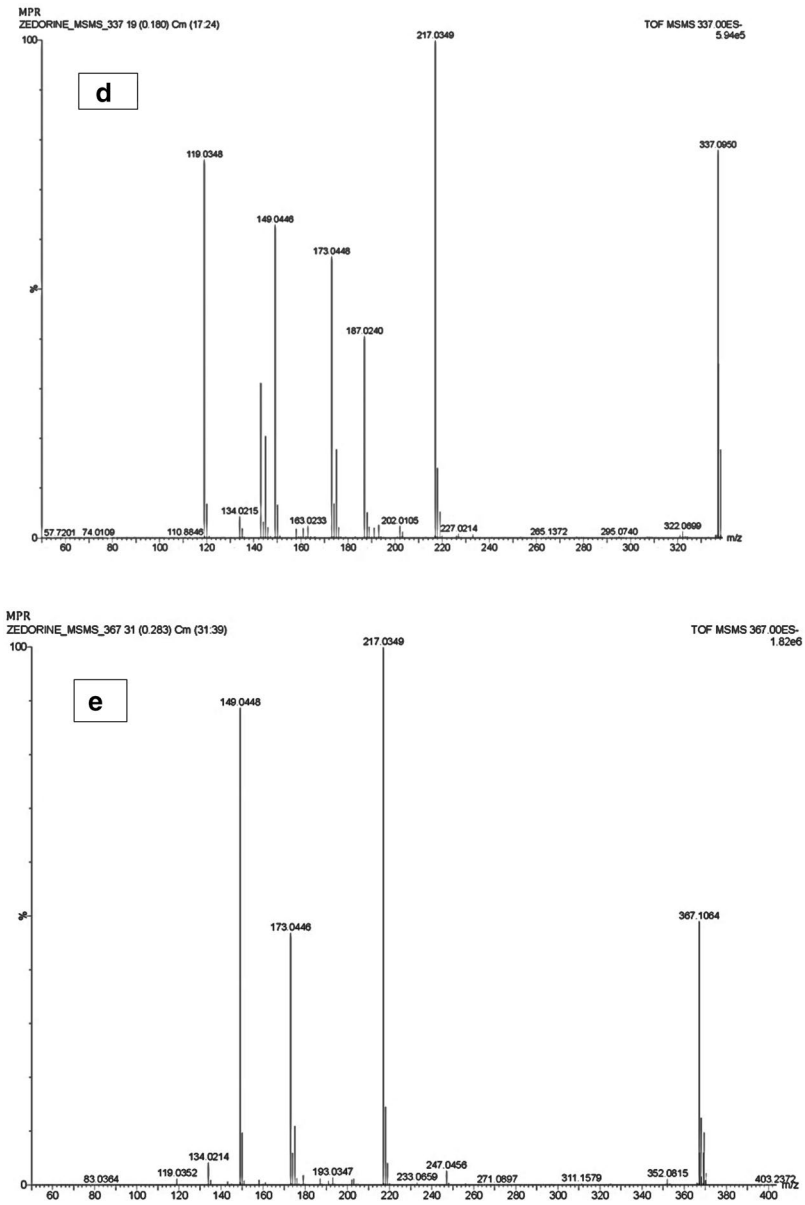

4.2.2 Field Emission-Scanning Electron Microscopy

The SEM micrographs (Fig. 5a, b) were obtained for phytoformulation containing nanosized ZnO particles and *C. zedoaria* extract at different magnifications. From this, the nanocomposite phytoformulation can be observed as uniform clusters as in Fig. 5 b [42]. The association between the metal oxide NP and *C. zedoaria* extract might have resulted in the formation of nanosized clusters [42].

4.3 Characterization of Nanoconjugate Loaded Microspheres

4.3.1 FE-SEM

The PCL microspheres could be clearly observed in the SEM micrographs (Fig. 6). They were observed to have good sphericity and were polydisperse with size ranging from 4 to 36 µm (Fig. 6a). On further magnification, the

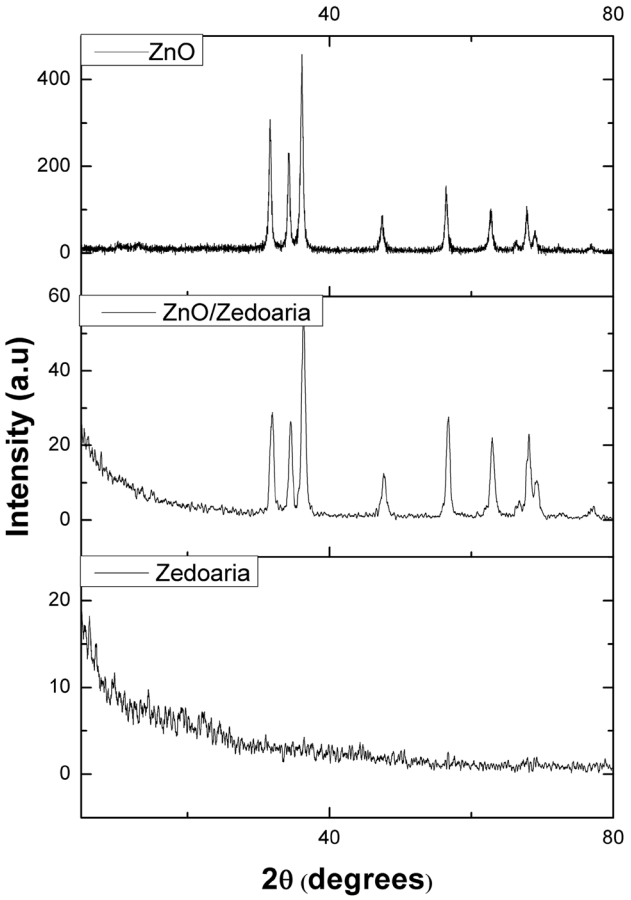

Fig. 4 XRD profiles of ZnO nanoparticle, *C. zedoaria* and ZnO/*C. zedoaria* nanocomposite showing the characteristic peaks of ZnO nanoparticle, *C. zedoaria* extract and the nanocomposite

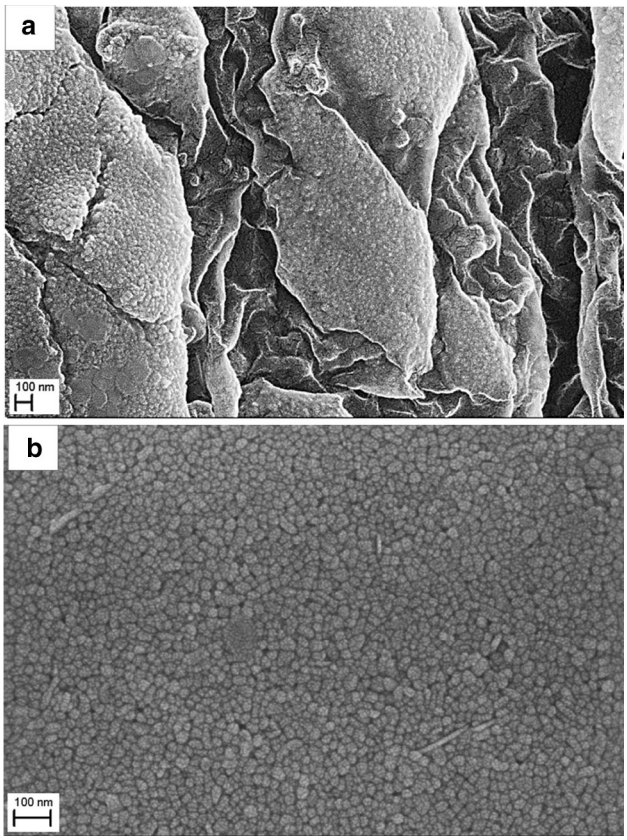

Fig. 5 FE-SEM micrographs of the prepared nanocomposite at lower and higher magnifications (**a, b**), the micrographs depict the uniform clusters of the nanocomposite material

surface of the microsphere appears to be covered with pores that vary in size from 49 to 640 nm. The surface of the microspheres also showed the unidirectional fibril formations characteristic of neat PCL (Fig. 6b, c) [31]. Solvent evaporation could induce fibrillary structures and nanosized pore on the surface of neat PCL microspheres (Fig. 6b, c). These are the result of crystallisation process of polymer during solvent evaporation, induced by chain diffusion [34].

The ZnO/*C. zedoaria* loaded microspheres (Fig. 6d) also appeared to be polydisperse with a size range of 6 to 39 µm. Their magnified surface morphology revealed the microsphere exterior to be speckled with white particles (Fig. 6e). These white particles on further magnification revealed structures similar to the ZnO/*C. zedoaria* nanocomposite (Fig. 6f). The pores and characteristic fibril formation on the surface of the microspheres loaded with nanocomposite were found to be absent when compared to the control [31]. From the SEM micrographs, the nanoconjugate particles appear to be coated on the surface of the microspheres (Fig. 6e). This preferential adhesion on the surface of the microspheres could be attributed to the hydrophilicity of the ZnO/*C. zedoaria* phytocomposite. This property of the phytonanocomposite has been demonstrated to be the basis of layer formation on the surface of PCL microspheres. This is also in accordance with the results published by Wang et al. where hydrophilic rhodamine was observed to be on the surface of PCL microspheres [43].

4.3.2 X-ray Diffraction (XRD)

The XRD profile of the neat PCL showed the characteristic reflection of the polymer at 2θ = 21.4° and 23.8°. The reflections at 2θ = 21.4° and 2θ = 23.8° indicated (110) and (200) planes in PCL respectively (Fig. 7). The presence of all the characteristic reflections in the XRD pattern of neat polymeric microspheres confirmed the microspheres to be composed of PCL. However, ZnO/*C. zedoaria* loaded PCL microspheres did not show any reflection corresponding to the polymer. ZnO/*C. zedoaria* loaded microspheres showed reflections for ZnO NPs at 2θ values = 31.6°, 34.2°, 36.1°, 47.4°, 56.5°, 62.7°, 66.3°, 67.8°, and 68.9°. The XRD diffraction patterns of *C. zedoaria* were also observed occurred at 2θ = 14.5°, 17.2°, 21.17°, 23.47° and 25.5° [13,

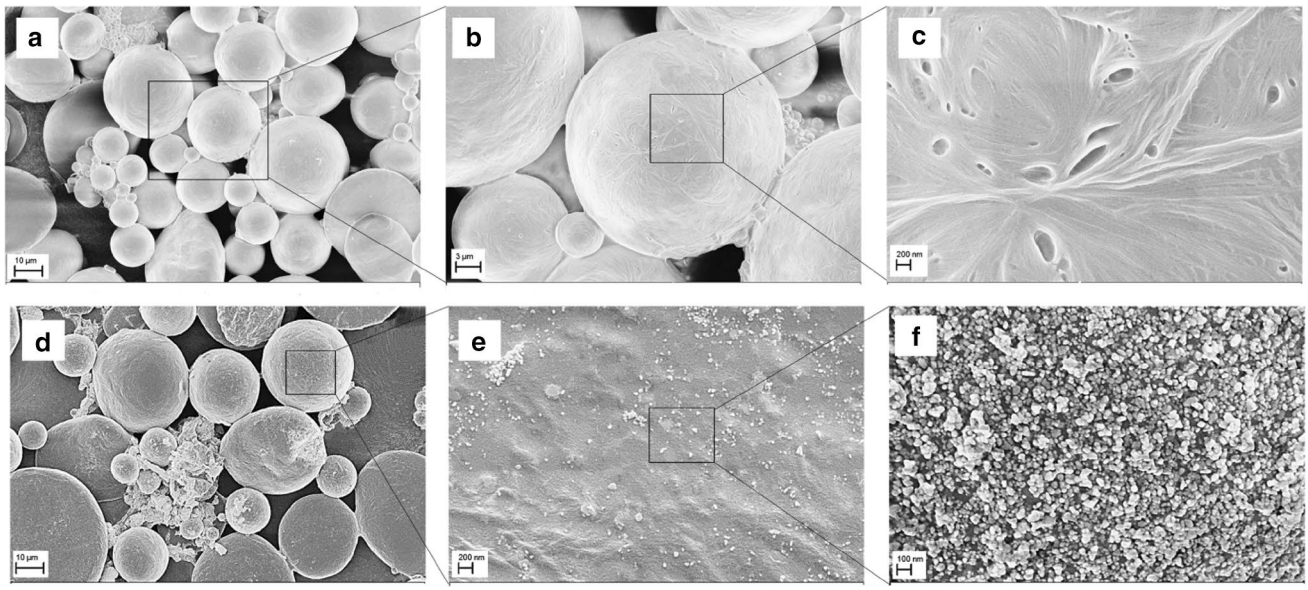

Fig. 6 FE-SEM micrographs of **a** Neat PCL microspheres, **b** microspheres at × 6000 magnification, **c** the surface of microspheres at × 50,000 magnification, **d** nanocomposite loaded microspheres, **e** surface of the microspheres at × 50,000, and **f** the nanocomposites

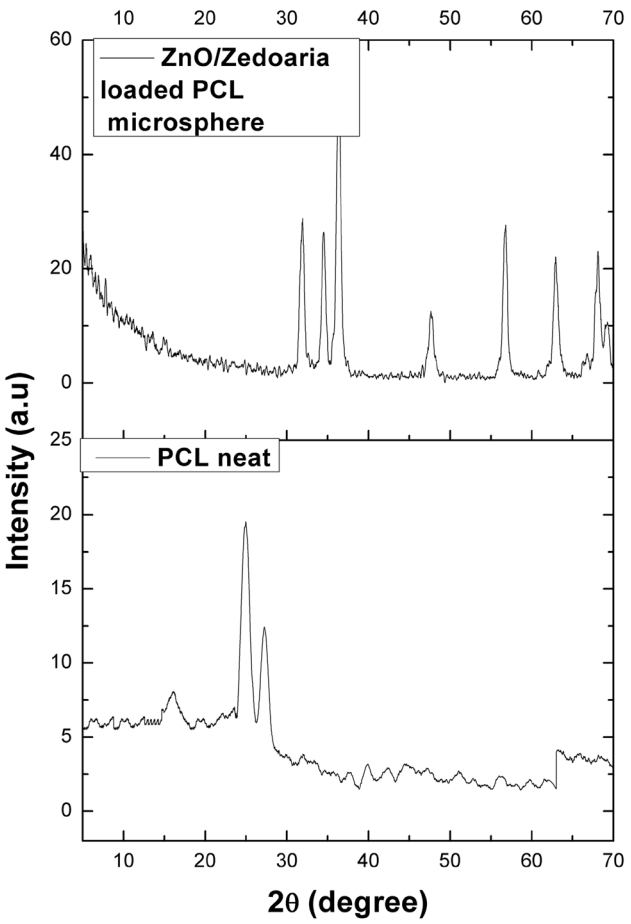

Fig. 7 XRD profiles of neat PCL and nanocomposite loaded microspheres with masked reflections of the polymer

34] (Fig. 7). This confirmed the presence of the ZnO/*C. zedoaria* nanocomposite on the surface of the PCL microbeads as observed by the FE-SEM micrographs. However, the absence of the PCL reflections in the XRD profile of the nanocomposite loaded microsphere could indicate the complete covering of microsphere surface by the nanocomposite phytoformulation thereby hindering the reflections from the semi crystalline planes of the polymeric material [34].

4.4 Antimicrobial Properties of ZnO/*C. zedoaria* Nanocomposite and PCL Microspheres

The prepared nanocomposite of ZnO and *C. zedoaria* were analysed for antimicrobial activity against *S. aureus* (Fig. 8). The conjugate showed promising antibacterial activity. ZnO and *C. zedoaria* extract separately showed a zone of inhibition of 11.3 and 11 mm respectively. Remarkably, the nanoconjugate produced an inhibition zone of 15 mm [3] (Table 2). Upon combining the metal oxide nanoparticle with the extract, a synergistic effect was observed which resulted in increased antimicrobial activity. This could be attributed to the combination of nanosized particle with the phyto-antimicrobial agent. The conjugation between these materials might have facilitated easier delivery of the plant based antimicrobials into the bacterial cells [44]. Along with this, the multi-targeted action of both ZnO and *C. zedoaria* extract might have provided the synergistic inhibitory effect. This could be the basis of the observed superior antimicrobial functioning of the nanocomposite.

The PCL microspheres were prepared as delivery vectors for the metal oxide-plant extract nanoconjugate.

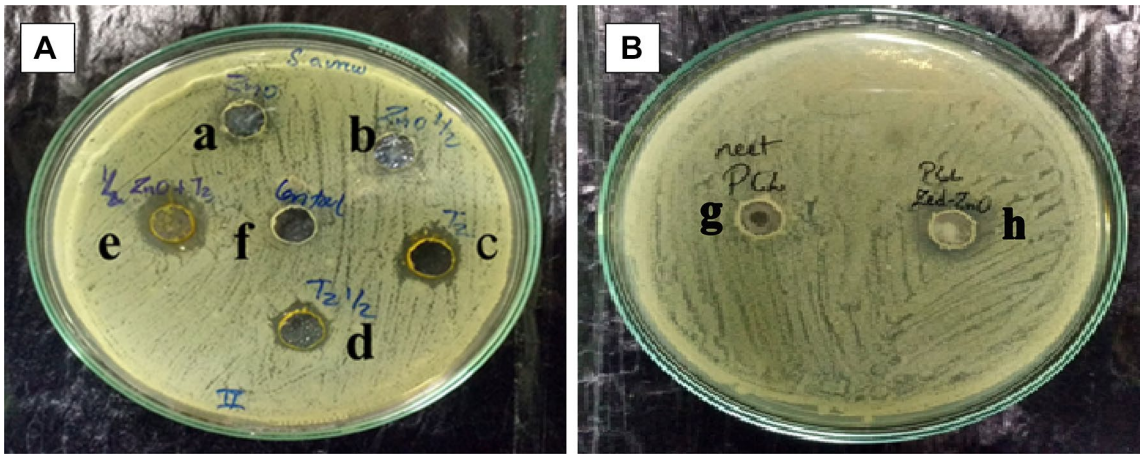

Fig. 8 **A** Antimicrobial activity against *S. aureus* by ZnO nanoparticles (a, b), *C. zedoaria* extract (c, d), nanocomposite of ZnO and *C. zedoaria* extract (e) and control (f). **B** Antimicrobial activity of microspheres against *S. aureus*. Neat PCL microspheres (g) and PCL/zedoaria/ZnO microspheres (h)

Table 2 Summary of the antimicrobial activity against *S. aureus*

S. no.	Sample	Inhibition zone (mm)
a, b	ZnO	11.3
d, c	Tz	11
e	ZnO + Tz	15
f	Control	–
g	Neat PCL	–
h	PCL/ZnO/zedoaria	15

Antimicrobial activity of these polymeric antimicrobial microspheres were tested on *S. aureus*. The PCL/ZnO/*C. zedoaria* microspheres showed remarkable antimicrobial property with an inhibition zone of 15 mm [45] (Fig. 8). The neat PCL microspheres did not show any antimicrobial activity as PCL doesn't have any inherent antimicrobial property. The nanocomposite loaded microspheres exhibited antimicrobial activity similar to that of the nanoconjugate. This could be explained by the presence of nanocomposite on the surface of the microspheres which directly acted against the microbes. According to the diffusion principle, there would be an initial burst release of the nanocomposite followed by sustained release from the microsphere surface [43]. Thus, the prepared ZnO/*C. zedoaria* loaded PCL microspheres could be very useful in applications where a quick and sustained antimicrobial activity is necessary. These microspheres can be used for eliminating pathogenic microbes from various fluids including the biological fluids and wound surfaces. The microspheres can be easily removed from the fluids by filtration or restrained in an appropriate membrane to unleash their antimicrobial activity.

5 Conclusion

Development of effective antimicrobials for in vivo as well as *ex vivo* applications is a matter of utmost importance, considering the rapidly evolving resistant species of pathogenic microbes. In this study, an effective antimicrobial nano-phytoformulation was synthesised and loaded onto a delivery vehicle for effective and prolonged release of the nano-phytoformulation. The *C. zedoaria* extract used in the study revealed the presence of various bioactive metabolites.

The prepared ZnO/*C. zedoaria* loaded PCL microspheres can be used as an effective antimicrobial in applications that require immediate and sustained release of effective antimicrobial. This preliminary study also opens up the opportunity to test the microspheres in living systems after further evaluation of the prepared microspheres.

Acknowledgements The authors would like to thank Department of Science and Technology (DST) the instrument facilities at International and Inter University Centre for Nanoscience and Nanotechnology and School of Biosciences, Mahatma Gandhi University.

Funding This research did not receive any specific grant from funding agencies in the public, commercial, or not-for-profit sectors.

Compliance with Ethical Standards

Conflict of interest The authors declare no conflict of interest.

References

1. N.D. Prajapati, *Handbook of Medicinal Plants* (Agrobios, Jodhpur, 2003)
2. K.I. Kim, J.W. Kim, B.S. Hong, D.H. Shin, H.Y. Cho, H.K. Kim et al., Antitumor, genotoxicity and anticlastogenic activities of polysaccharide from *Curcuma zedoaria*. Mol. Cells **10**(4), 392–398 (2000)
3. B. Wilson, G. Abraham, V. Manju, M. Mathew, B. Vimala, S. Sundaresan et al., Antimicrobial activity of *Curcuma zedoaria* and *Curcuma malabarica* tubers. J. Ethnopharmacol. **99**(1), 147–151 (2005)
4. B.V. Bonifácio, P.B. da Silva, dos M.A. Santos Ramos, K.M.S. Negri, T.M. Bauab, M. Chorilli, Nanotechnology-based drug delivery systems and herbal medicines: a review. Int. J. Nanomed. **9**, 1 (2014)
5. S. Ansari, M. Farha Islam, Influence of nanotechnology on herbal drugs: a review. J. Adv. Pharm. Technol. Res. **3**(3), 142 (2012)
6. A. Abbasi, J.J. Sardroodi, A highly sensitive chemical gas detecting device based on N-doped ZnO as a modified nanostructure media: a DFT + NBO analysis. Surf. Sci. **668**, 150–163 (2018)
7. A. Abbasi, J.J. Sardroodi, An innovative gas sensor system designed from a sensitive nanostructured ZnO for the selective detection of SO x molecules: a density functional theory study. New J. Chem. **41**(21), 12569–12580 (2017)
8. A. Abbasi, J.J. Sardroodi, Modified N-doped TiO_2 anatase nanoparticle as an ideal O_3 gas sensor: insights from density functional theory calculations. Comput. Theor. Chem. **1095**, 15–28 (2016)
9. A. Abbasi, J.J. Sardroodi, Investigation of the adsorption of ozone molecules on TiO_2/WSe_2 nanocomposites by DFT computations: applications to gas sensor devices. Appl. Surf. Sci. **436**, 27–41 (2018)
10. A. Abbasi, J.J. Sardroodi, N-doped TiO_2 anatase nanoparticles as a highly sensitive gas sensor for NO_2 detection: insights from DFT computations. Environ. Sci.: Nano **3**(5), 1153–1164 (2016)
11. A.I. El-Batal, F.M. Mosalam, M. Ghorab, A. Hanora, A.M. Elbarbary, Antimicrobial, antioxidant and anticancer activities of zinc nanoparticles prepared by natural polysaccharides and gamma radiation. Int. J. Biol. Macromol. **107**, 2298–2311 (2018)
12. S.I. Hong, P. Ganeshan, A. Vincent, S. Mahalingam, Green synthesis and characterization of zinc oxide nanoparticle antimicrobial anticancer activity using insulin plant (*Costus pictus* D. Don) leaf extract. Adv. Nat. Sci.: Nanosci. Nanotechnol. https://doi.org/10.1088/issn.2043-6262
13. K. Soumya, S. Snigdha, S. Sugathan, J. Mathew, E. Radhakrishnan, Zinc oxide–curcumin nanocomposite loaded collagen membrane as an effective material against methicillin-resistant coagulase-negative *Staphylococci*. 3 Biotech **7**(4), 238 (2017)
14. B. Prakash, Use of metals in Ayurvedic medicine. Indian J. Hist. Sci. **32**, 1–28 (1997)
15. K. Ali, S. Dwivedi, A. Azam, Q. Saquib, M.S. Al-Said, A.A. Alkhedhairy et al., *Aloe vera* extract functionalized zinc oxide nanoparticles as nanoantibiotics against multi-drug resistant clinical bacterial isolates. J. Colloid Interface Sci. **472**, 145–156 (2016)
16. K. Joshy, S. Snigdha, G. Anne, K. Nandakumar, T. Sabu, Poly (vinyl pyrrolidone)-lipid based hybrid nanoparticles for anti viral drug delivery. Chem. Phys. Lipids **210**, 82–89 (2018)
17. J. Yang, F. Gao, D. Han, L. Yang, X. Kong, M. Wei et al., Multifunctional zinc-based hollow nanoplatforms as a smart pH-responsive drug delivery system to enhance in vivo tumor-inhibition efficacy. Mater. Des. **139**, 172–180 (2018)
18. M. Rampichová, M. Buzgo, V. Lukášová, A. Míčková, K. Vocetková, V. Sovková et al. Functionalization of 3D fibrous scaffolds prepared using centrifugal spinning with liposomes as a simple drug delivery system. Acta Polytech. CTU Proc. **8**, 24–26 (2017)
19. B. Rai, S.-H. Teoh, D. Hutmacher, T. Cao, K. Ho, Novel PCL-based honeycomb scaffolds as drug delivery systems for rhBMP-2. Biomaterials **26**(17), 3739–3748 (2005)
20. C.G. Pitt, A.R. Jeffcoat, R.A. Zweidinger, A. Schindler, Sustained drug delivery systems. I. The permeability of poly (ε-caprolactone), poly (DL-lactic acid), and their copolymers. J. Biomed. Mater. Res. **13**(3), 497–507 (1979)
21. J. Kundu, J.H. Shim, J. Jang, S.W. Kim, D.W. Cho, An additive manufacturing-based PCL–alginate–chondrocyte bioprinted scaffold for cartilage tissue engineering. J. Tissue Eng. Regen. Med. **9**(11), 1286–1297 (2015)
22. F. Wang, Y. Xu, C. Lv, C. Han, Y. Li, Enhanced wound healing activity of PEG/PCL copolymer combined with bioactive nanoparticles in wound care after anorectal surgery: via bio-inspired methodology. J. Photochem. Photobiol. B: Biol. **187**, 54–60 (2018)
23. J.P. Temple, D.L. Hutton, B.P. Hung, P.Y. Huri, C.A. Cook, R. Kondragunta et al., Engineering anatomically shaped vascularized bone grafts with hASCs and 3D-printed PCL scaffolds. J. Biomed. Mater. Res. Part A **102**(12), 4317–4325 (2014)
24. J. Yang, S.-B. Park, H.-G. Yoon, Y.-M. Huh, S. Haam, Preparation of poly ε-caprolactone nanoparticles containing magnetite for magnetic drug carrier. Int. J. Pharm. **324**(2), 185–190 (2006)
25. J. Chen, W. Que, Y. Xing, B. Lei, Molecular level-based bioactive glass-poly (caprolactone) hybrids monoliths with porous structure for bone tissue repair. Ceram. Int. **41**(2), 3330–3334 (2015)
26. X. Zeng, W. Tao, L. Mei, L. Huang, C. Tan, S.-S. Feng, Cholic acid-functionalized nanoparticles of star-shaped PLGA-vitamin E TPGS copolymer for docetaxel delivery to cervical cancer. Biomaterials **34**(25), 6058–6067 (2013)
27. J.E. Song, A.R. Kim, C.J. Lee, N. Tripathy, K.H. Yoon, D. Lee et al., Effects of purified alginate sponge on the regeneration of chondrocytes: in vitro and in vivo. J. Biomater. Sci. Polym. Ed. **26**(3), 181–195 (2015)
28. D. Zhu, W. Tao, H. Zhang, G. Liu, T. Wang, L. Zhang et al., Docetaxel (DTX)-loaded polydopamine-modified TPGS-PLA nanoparticles as a targeted drug delivery system for the treatment of liver cancer. Acta Biomater. **30**, 144–154 (2016)
29. N. Gao, Z. Chen, X. Xiao, C. Ruan, L. Mei, Z. Liu et al., Surface modification of paclitaxel-loaded tri-block copolymer PLGA-b-PEG-b-PLGA nanoparticles with protamine for liver cancer therapy. J. Nanopart. Res. **17**(8), 347 (2015)
30. R. Li, C. Xiang, M. Ye, H.-F. Li, X. Zhang, D.-A. Guo, Qualitative and quantitative analysis of curcuminoids in herbal medicines derived from *Curcuma* species. Food Chem. **126**(4), 1890–1895 (2011)
31. A. Mukerjee, V. Sinha, V. Pruthi, Preparation and characterization of poly-ε-caprolactone particles for controlled insulin delivery. J. Biomed. Pharm. Eng. **1**(1), 40–44 (2007)
32. J.M. Halket, D. Waterman, A.M. Przyborowska, R.K. Patel, P.D. Fraser, P.M. Bramley, Chemical derivatization and mass spectral libraries in metabolic profiling by GC/MS and LC/MS/MS. J. Exp. Bot. **56**(410), 219–243 (2004)
33. S. Mathew, S. Snigdha, J. Mathew, E. Radhakrishnan, Poly (vinyl alcohol): Montmorillonite: boiled rice water (starch) blend film reinforced with silver nanoparticles; characterization and antibacterial properties. Appl. Clay Sci. **161**, 464–473 (2018)
34. S.S. Babu, N. Kalarikkal, S. Thomas, E. Radhakrishnan, Enhanced antimicrobial performance of cloisite 30B/poly (ε-caprolactone) over cloisite 30B/poly (L-lactic acid) as evidenced by structural features. Appl. Clay Sci. **153**, 198–204 (2018)

35. S. Uehara, I. Yasuda, K. Takeya, H. Itokawa, Terpenoids and curcuminoids of the rhizoma of *Curcuma xanthorrhiza* Roxb. Yakugaku Zasshi: J. Pharm. Soc. Jpn **112**(11), 817–823 (1992)
36. I. Sasidharan, A.N. Menon, Comparative chemical composition and antimicrobial activity fresh & dry ginger oils (*Zingiber officinale* Roscoe). Int. J. Curr. Pharm. Res. **2**(4), 40–43 (2010)
37. J.M. Halket, D. Waterman, A.M. Przyborowska, R.K.P. Patel, P.D. Fraser, P.M. Bramley, Chemical derivatization and mass spectral libraries in metabolic profiling by GC/MS and LC/MS/MS. J. Exp. Bot. **56**(410), 219–243 (2005)
38. Y. Cao, R.X. Xu, Z. Liu, A high-throughput quantification method of curcuminoids and curcumin metabolites in human plasma via high-performance liquid chromatography/tandem mass spectrometry. J. Chromatogr. B **0**, 70–78 (2014)
39. K.-Y. Yang, L.-C. Lin, T.-Y. Tseng, S.-C. Wang, T.-H. Tsai, Oral bioavailability of curcumin in rat and the herbal analysis from *Curcuma longa* by LC–MS/MS. J. Chromatogr. B **853**(1–2), 183–189 (2007)
40. R.P. Singh, D. Jain, Evaluation of antimicrobial activity of curcuminoids isolated from turmeric. Int. J. Pharm. Life Sci. **3**(1), 1368–1376 (2012)
41. L. Ambarsari, W. Nurcholis, L.K. Darusman, M.A. Mujib, R. Heryanto, The curcuminoids extract of *Curcuma xanthorriza* roxb loaded solid lipid nanoparticles. Int. J. Sci. Res. **3**(10), 852–856 (2014)
42. G. Baskar, A. Gurugulladevi, T. Nishanthini, B.G. Garrick, R. Aiswarya, M. Gopinath, Synthesis of phytonanocomposite of zinc oxide by *Ixora coccinea* Linn for Cancer treatment. J. Inorg. Organomet. Polym Mater. **26**(4), 876–880 (2016)
43. X. Wang, Y. Wang, K. Wei, N. Zhao, S. Zhang, J. Chen, Drug distribution within poly (ε-caprolactone) microspheres and in vitro release. J. Mater. Process. Technol. **209**(1), 348–354 (2009)
44. R. Lobo, K.S. Prabhu, A. Shirwaikar, A. Shirwaikar, *Curcuma zedoaria* Rosc.(white turmeric): a review of its chemical, pharmacological and ethnomedicinal properties. J. Pharm. Pharmacol. **61**(1), 13–21 (2009)
45. J.P. Raval, D.R. Naik, K.A. Amin, P.S. Patel, Controlled-release and antibacterial studies of doxycycline-loaded poly (ε-caprolactone) microspheres. J. Saudi Chem. Soc. **18**(5), 566–573 (2014)